

# A study of kidney parameters in mice induces by super magnetic Fe<sub>3</sub>O<sub>4</sub> nanoparticles capped with PEG

Abdulkadhim Waleed<sup>1</sup>, Jabir Majid<sup>2\*</sup> and Nayef Uday<sup>1</sup>

1. Department of Applied Science, Division of Applied Physics, University of Technology, Baghdad, IRAQ

2. Department of Applied Science, Division of Biotechnology, University of Technology, Baghdad, IRAQ

\*msj\_iraq@yahoo.com

## Abstract

The magnetite nanoparticles Fe<sub>3</sub>O<sub>4</sub> capped with polyethylene glycol PEG were prepared by hydrothermal method. Due to the successful coating of PEG molecules on the surface of Fe<sub>3</sub>O<sub>4</sub>, these nanoparticles exhibited excellent dispersibility and dissolvability in physiological condition. The obtained nanoparticles were characterized by transmission electron microscopy (TEM), Fourier transform infrared (FTIR) spectroscopy and vibrating sample magnetometer (VSM). The Fe<sub>3</sub>O<sub>4</sub> nanoparticles size is 17 nm while PEG-Fe<sub>3</sub>O<sub>4</sub> size is 4nm and exhibited superparamagnetism and high saturation magnetization at room temperature.

However, the available data on their *in vivo* toxicity are limited. The present study was aimed to evaluate the toxicity of Fe<sub>3</sub>O<sub>4</sub>, PEG-Fe<sub>3</sub>O<sub>4</sub> using both morphological and functional criteria. The biochemical parameters were assessed *in-vivo* using animal model. MNPs were injected intraperitoneal for 7, 14, 21 and 28 day. Furthermore, the histological structure of kidney samples was examined. Our results show no significant changes in biochemical parameters. The histological remained unchanged through the entire observation period time. The body weight was non-significant change through long period after administration of MNPs.

**Keywords:** PEG-Fe<sub>3</sub>O<sub>4</sub>, Hydrothermal synthesis, MNPs side effect, Superparamagnetic.

## Introduction

The nanoparticles have more of specific physical and chemical characters in relation to their shape, size and high proportion in the surface to volume. Where these characters are present, make them appropriate for the use in multiple biology and medical applications like contrast media to drug delivery<sup>17</sup>, tissue repair, cellular therapy<sup>19</sup>, immunoassays<sup>1</sup>, hyperthermia<sup>4</sup> and magnetic resonance imaging<sup>20</sup>. The nanoparticles consist of elements like nickel, iron and cobalt exhibiting magnetic properties and are called magnetic nanoparticles. The developments and works on novel process in fields of tumors hyperthermia are be more studied. For the development, the nanoparticles composite use such as core-shell superparamagnetic particles have combined advantage from hetero-materials. Polyethylene glycol (PEG)

coating nanoparticles and Fe<sub>3</sub>O<sub>4</sub> nanoparticles all of particulars interest for having not only magnetism in Fe<sub>3</sub>O<sub>4</sub>.

Fe<sub>3</sub>O<sub>4</sub> and Fe<sub>2</sub>O<sub>3</sub> magnetic nanoparticle are used as satisfactory thermal therapeutic on cells line and animals model of kidney cancer and liver cancer in magnetic fluid hyperthermia (MFH), not with histological toxicity in the tissues or organs<sup>5,21</sup>. In these present studies, high crystalline and monodispersed core-shell multifunction PEG-Fe<sub>3</sub>O<sub>4</sub> composite magnetic nanoparticles were synthesized and used in magnetic fluid hyperthermia as combined with near-inferred hyperthermia. Formation of the core-shell structure is achieved in two consecutive steps, where the Fe<sub>3</sub>O<sub>4</sub> core is coated by the PEG shell. Good engineering PEG-Fe<sub>3</sub>O<sub>4</sub> composite magnetic nanoparticles tend to aggregate in the tumors due to the unorganized nature of malignancy vasculature.

The nature in the composite PEG-Fe<sub>3</sub>O<sub>4</sub> (MNPs) can show to have biocompatibility. The biocompatibility and the toxicity in both (*in vivo* and *in vitro*) are needed to evaluate. Thus, hemolysis test, the cytotoxicity assay, micronucleus assay and detection of very toxicity in mice are introduced to evaluate the biocompatibility in self-assemble PEG-Fe<sub>3</sub>O<sub>4</sub> composite magnetic nanoparticles in these researches.<sup>6,22</sup>

## Material and Methods

**Chemicals and Materials:** Anhydrous sodium acetate (NaOAc), ethylene glycol (EG), polyethylene glycol (PEG-4000), ethanalamine (ETA), ethanol and ferric chloride hexahydrate (FeCl<sub>3</sub>·6H<sub>2</sub>O) were supplied by Beijing Chemicals (China) while Calcein AM was procured from Sigma-Aldrich (Shanghai, China).

**Preparation of Fe<sub>3</sub>O<sub>4</sub>-PEG MNPs:** Fe<sub>3</sub>O<sub>4</sub> – PEG MNPs were synthesized by hydrothermal method. 3gm of FeCl<sub>3</sub>·6H<sub>2</sub>O was dissolved in 40ml of solvent containing EG 20ml and ETA 20ml to form a stable orange solution. NaOAc 4.0g and PEG-4000 2.0g were added into the above solution under magnetic stirring. The homogeneous solution was transferred to a Teflon-lined stainless-steel autoclave 100ml and sealed to heat at 200°C. After 10 hrs., the autoclave was cooled to ambient temperature naturally. The magnetic nanoparticles were washed with ethanol and DW in sequence and then dried in vacuum at 60°C overnight.

**Characterisation of PEG-Fe<sub>3</sub>O<sub>4</sub> MNPs:** The prepared magnetite nanoparticles (MNPs) were characterized via optical and structural techniques. The TEM samples were prepared by placing a drop of the MNP solution on a gold-

coated Cu grid containing about 200 meshes. Transmission electron microscope (TEM; Philips) was used to examine the morphological features of the MNPs. The molecular vibrations of the samples were studied using 8000 Series Shimadzu FTIR spectroscopy system. The magnetic properties of  $\text{Fe}_3\text{O}_4$  NPs were determined using a BVH-55 vibrating sample magnetometer (VSM).

### Toxicity of PEG- $\text{Fe}_3\text{O}_4$ MNPs

**Animal body weight Examination:** The mice were of age between 6-8 weeks and have weight from 25-33 gram. The mice were divided in to three groups: First group: the mice injected with the physiological phosphate solution (PBS) as a negative control. Second group: injected with 1 mg/kg with bare  $\text{Fe}_3\text{O}_4$ . Third group: injected with 1 mg/kg with  $\text{Fe}_3\text{O}_4$  - PEG MNPs, all animals group were left for 1, 2, 3 and 4 weeks. After end of experiment time, the body weight of animal lab was measured.<sup>15</sup>

**Assessment of Biochemical Serum Markers:** Blood was drawn from the heart through the heart puncture to obtain the largest quantity of blood. Whole blood was collected using universal tubes and then centrifuged at 3500rpm for 10min in order to separate serum. Using a biochemical analyzer (Chemistry Analyzer, Automated, Abbott Laboratories and Architect c4000), serum biochemical analysis was carried out to measure blood urea and creatinine in order to evaluation kidney function.

**Histopathological Examination:** The kidney samples were fixed in buffered (10%) par formaldehyde, embedded in paraffin, cut into (5 $\mu\text{m}$ ) sections and stained with hematoxylin and eosin (H and E) for histological examination using standard techniques. After H and E staining, the slides were observed and photos were taken using an optical microscope at 100 $\times$ .

**Statistical analysis:** The obtained data were statically analyzed by unpaired t.test with GraphPad Prism 6. The values were shown as the Mean  $\pm$  SEM of triplicate of each experiment.<sup>14</sup>

## Results and Discussion

### Morphological properties of PEG- $\text{Fe}_3\text{O}_4$ MNPs

**Transmission Electron Microscopy (TEM):** The particles size and morphology of magnetite nanoparticles samples were investigated using TEM as shown in fig. 1. The particles are approximate spherical shape and the average diameter for  $\text{Fe}_3\text{O}_4$  was 17 nm while PEG- $\text{Fe}_3\text{O}_4$  size was 4nm. Our results show that the PEG- $\text{Fe}_3\text{O}_4$  MNPs are less agglomerated from  $\text{Fe}_3\text{O}_4$ . The less agglomerated texture of the PEG- $\text{Fe}_3\text{O}_4$  can be related to the effect of polymer layer during the particle formation and using more concentration of ( $\text{FeCl}_3 \cdot 6\text{H}_2\text{O}$ ). Then, PEG coating reduced in size and aggregation and the particles dispersion got better.

**Chemical properties of PEG- $\text{Fe}_3\text{O}_4$  MNPs:** The FTIR spectra of the  $\text{Fe}_3\text{O}_4$ -PEG MNPs are shown in fig. 2. Our

results showed the broad peak near 3431.48 or 3450.77  $\text{cm}^{-1}$  in all FTIR spectra belong to attached hydroxyl groups.<sup>22</sup> The absorption bands around 1620.26 $\text{cm}^{-1}$  originate from stretching and deformation vibration hydroxyl groups connected to the surface of nanoparticles. Also, the C-O-C ether stretch and vibration bands exist at 976.01 and 1043.52 or 1039.67 $\text{cm}^{-1}$  respectively. Also, the bands around 2922.25 $\text{cm}^{-1}$  correspond to -CH stretching vibration and its out-of-plane bending vibration respectively.

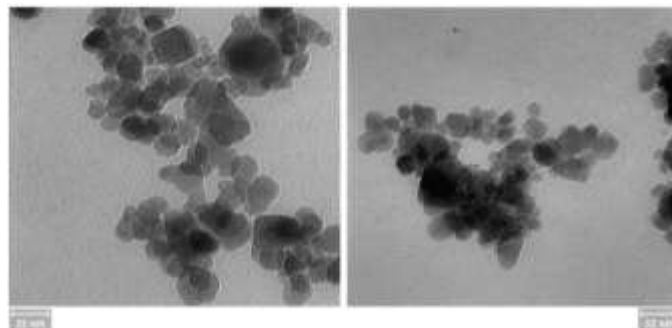


**Fig. 1: TEM images of  $\text{Fe}_3\text{O}_4$  and  $\text{Fe}_3\text{O}_4$ -PEG magnetic NP**

The -CH-groups bending are also observed at 1462 or 1464.02 $\text{cm}^{-1}$ . All these bands confirmed the existence of PEG in the product. The results exhibit metal-oxygen band at 580.59 or 584.45 $\text{cm}^{-1}$  corresponding to intrinsic stretching vibrations of the metal at tetrahedral site (Fe-tetra-O) whereas metal-oxygen band observed at 426.28 $\text{cm}^{-1}$ , is assigned to octahedral-metal stretching (Fe-octa-O).

**Vibrating sample magnetometer (VSM):** The magnetic properties for the  $\text{Fe}_3\text{O}_4$ -PEG MNPs were characterized by vibrating sample magnetometer (VSM). Figure 3 shows the typical at room temperature magnetization curves of PEG coated  $\text{Fe}_3\text{O}_4$  MNPs. Reduced magnetization in magnetic nanoparticles is often observed due to the increase of surface to volume ratio. With reduction of particle size and agglomeration, spin relaxation of domain increases and consequently, magnetization decreases. The absence of hysteresis and remanance implies that our nanoparticles have superparamagnetic features.

The saturation magnetization ( $M_s$ ) values of samples  $\text{Fe}_3\text{O}_4$ -PEG are 42.5 and 51emu/g respectively. The significant softening in magnetic properties occurred by PEG-coating onto the  $\text{Fe}_3\text{O}_4$  MNPs. The coercivity ( $H_c$ ) and the saturation magnetization ( $M_s$ ) of the MNPs increased with increasing particle size. The soft magnetic material is especial important in the biomedical fields, these PEG-coated soft magnetic  $\text{Fe}_3\text{O}_4$  MNPs may find good applications in the biological studies.

**Toxicity of PEG- $\text{Fe}_3\text{O}_4$  MNPs:** The body weight of mice and the total white blood cell (WBCs) count was unaffected after intraperitoneal exposure to  $\text{Fe}_3\text{O}_4$ , PEG- $\text{Fe}_3\text{O}_4$  MNPs for 4 weeks (fig. 4). Our results show no significant

differences in the urea concentration as well as creatinine in serum of injected for period of 1 week to 4 weeks (fig. 5).

However, histopathological examination of mouse tissue from control and treated groups has been done. The tissues of control and treated groups showed no significant pathological changes in the kidney (fig. 6). Our results show no changes in the kidney nodules. The kidney tissue also appeared as normal when compared with control untreated animals. No atrophy of the glomerular and renal tubular epithelial cells has been found in the kidneys.

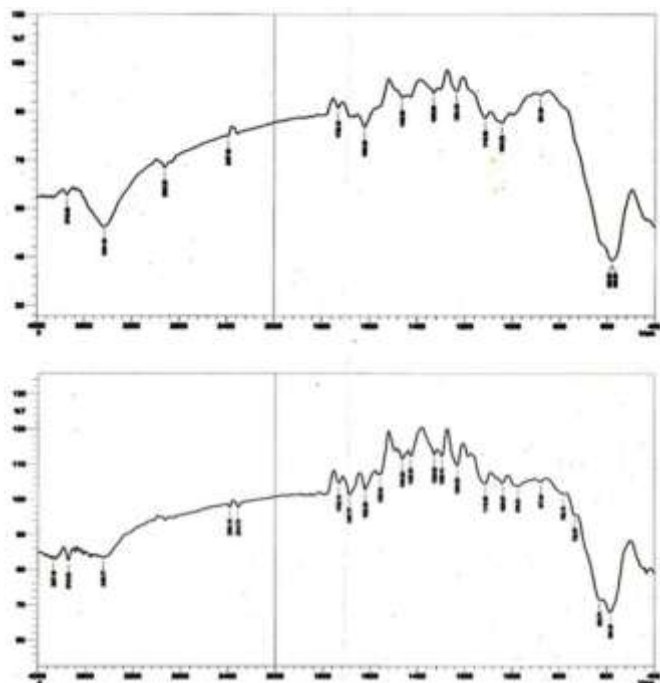


Fig. 2: FTIR spectra of Fe<sub>3</sub>O<sub>4</sub> and Fe<sub>3</sub>O<sub>4</sub>-PEG magnetic NPs

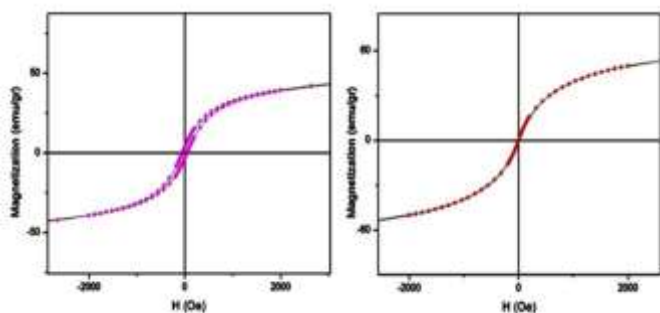


Fig. 3: VSM properties of Fe<sub>3</sub>O<sub>4</sub>, Fe<sub>3</sub>O<sub>4</sub>-PEG magnetic NPs

The exposure to Fe<sub>3</sub>O<sub>4</sub>, PEG-Fe<sub>3</sub>O<sub>4</sub> MNPs did not induce any histopathological changes in treated lab animals. The effects of injection of Fe<sub>3</sub>O<sub>4</sub> -PEG MNPs on blood urea and creatinine concentration are shown in fig. 6, the results showed no significant differences between the injected group and the control group during the 4 weeks. In conclusion, the PEG coated magnetite are biocompatible magnetic nanoparticles. The intravenous administration of

PEG-Fe<sub>3</sub>O<sub>4</sub> MNPs is done at a dose of 1 mg/kg, where any changes in serum biochemical markers or Histological on long period are not observed in 28 days after infusion. Body weights were not different after PEG-Fe<sub>3</sub>O<sub>4</sub>-treated animals. All these results are taken into consideration during the design of novel drug delivery systems.

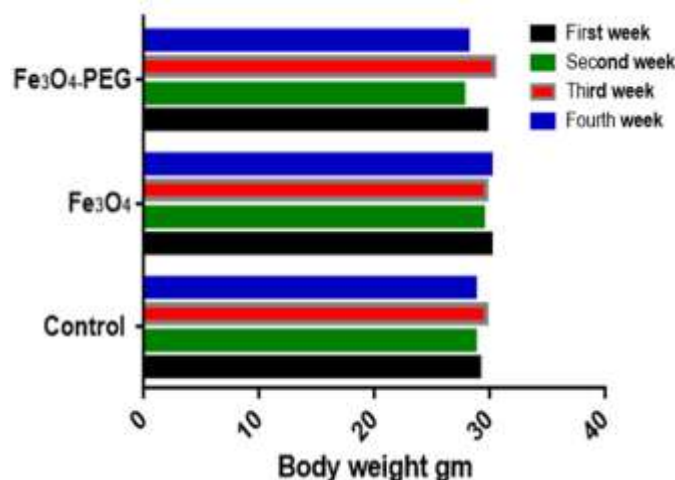


Fig. 4: Animals body weight after intraperitoneal injection of Fe<sub>3</sub>O<sub>4</sub>, Fe<sub>3</sub>O<sub>4</sub>-PEG MNPs.

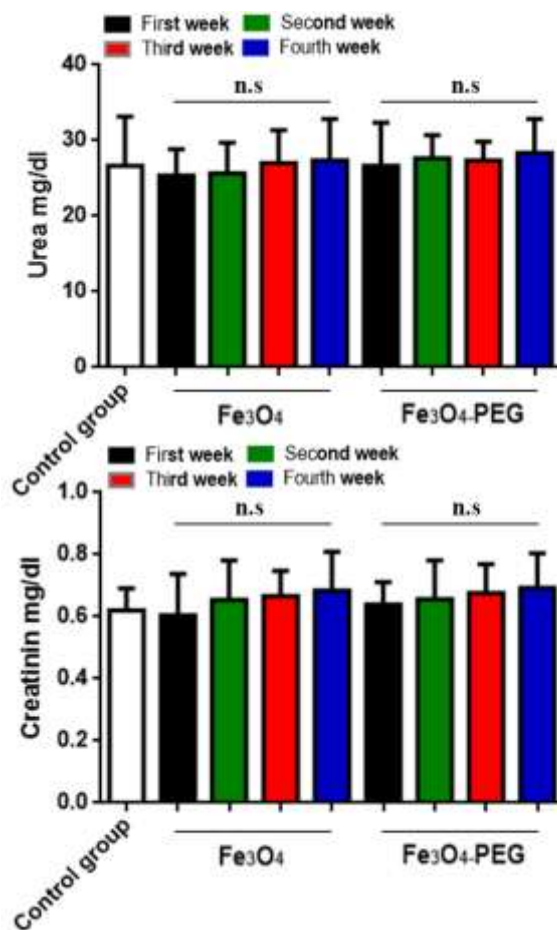
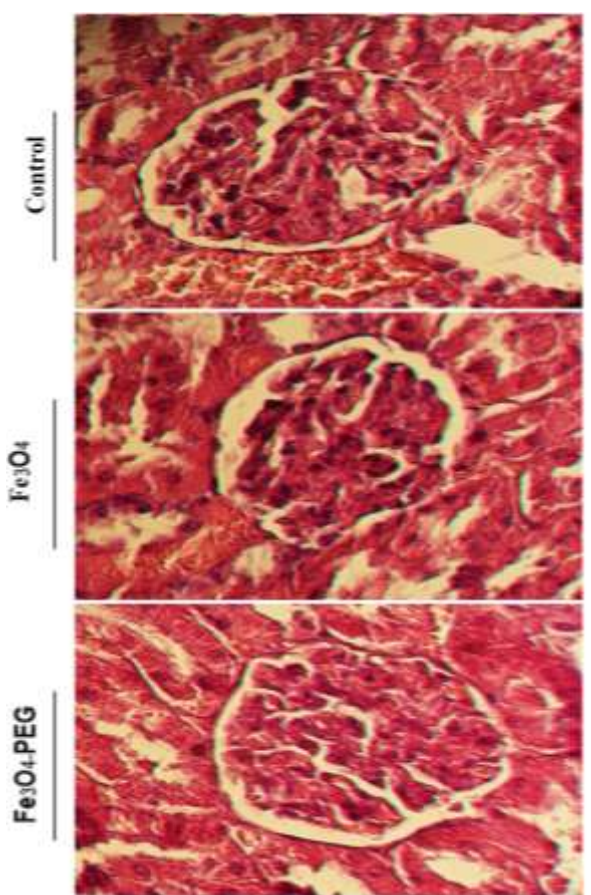


Fig. 5: Urea and creatinine level after intraperitoneal injection of Fe<sub>3</sub>O<sub>4</sub>, Fe<sub>3</sub>O<sub>4</sub>-PEG MNPs



**Figure 6: Kidney histological section after intraperitoneal injection of  $\text{Fe}_3\text{O}_4$ ,  $\text{Fe}_3\text{O}_4$ -PEG MNPs**

## References

- André C.S., Tiago R.O., Javier B.M., Suzana M.F., Luciana M., Lorena F.P., Tatiana T.S., Edson A., Alberto T., Edson L.G., Mateus J.M., Ricardo S.S. and Lionel F.G., Application of hyperthermia induced by superparamagnetic iron oxide nanoparticles in glioma treatment, *Int. J. Nanomedicine*, **6**, 591–603 (2011)
- Ajordan R.S. et al, Effects of magnetic fluid hyperthermia (MFH) on C3H mammary carcinoma in vivo, *Int. J. Hyperthermia*, **13**, 587–605 (1997)
- Anindita M., Nidhi J., Krishnananda C., Goutam D. and Facile A., Synthesis of PEG-Coated Magnetite ( $\text{Fe}_3\text{O}_4$ ) Nanoparticles and Their Prevention of the Reduction of Cytochrome C, *ACS Appl. Mater. Interfaces*, **4**, 142–149 (2012)
- Chenjie X., Luye M., Isaac R., David M., Matthias N., James A., Weian Z. and Jeffrey M., Nanoparticle-based monitoring of cell therapy, *Nanotechnology*, **22**, 494001 (2011)
- Du Y., Zhang D., Liu H. and Lai R., Thermochemotherapy effect of nanosized  $\text{As}_2\text{O}_3/\text{Fe}_3\text{O}_4$  complex on experimental mouse tumors and its influence on the expression of CD44v6, VEGF-C and MMP-9, *BMC Biotechnol*, **9**, 84 (2009)
- Daozhen C., Qiusha T., Xiangdong L., Xiaojin Z., Jia Z., Wen-Qun X., Jing-Ying X. and Cai-Qin G., Biocompatibility of magnetic  $\text{Fe}_3\text{O}_4$  nanoparticles and their cytotoxic effect on MCF-7 cells, *Int J. Nanomedicine*, **7**, 4973–4982 (2012)
- Zhao D., Teng P., Xu T., Xia Q. and Tang T., Simple hydrothermal synthesis of  $\text{Fe}_3\text{O}_4$ -PEG nanocomposite, *J. Alloys Compd*, **502**, 392 (2010)
- Gupta A. and Gupta M., Synthesis and surface engineering of iron oxide nanoparticles for biomedical applications, *Biomaterials*, **26**, 3995–4021 (2005)
- Jin L., Quan F., Masatsugu S., Itsuko S., Suzuki M., Engelhard H., Yuehe L., Nam K., Wang Jian Q. and Chuan-Jian Z., Monodispersed core-shell  $\text{Fe}_3\text{O}_4$ @Au nanoparticles, *J Phys Chem B*, **109**, 21593–21601 (2005)
- Jin H. and Kang K., Application of novel metal nanoparticles as optical/thermal agents in optical mammography and hyperthermic treatment for breast cancer, *Adv Exp Med Biol*, **599**, 45–52 (2007)
- Kirkpatrick C., Bittinger F., Wagner M., Köhler H., van Kooten T., Klein C. and Otto M., Current trends in biocompatibility testing, *Proc Inst Mech Eng H*, 75–84 (1998)
- Kouassi G. and Irudayaraj J., Magnetic and gold-coated magnetic nanoparticles as a DNA sensor, *Anal Chem*, **78**, 3234–3241 (2006)
- Liu H., Sonn C., Wu J., Lee K. and Kim Y., Synthesis of streptavidin FITC-conjugated core-shell  $\text{Fe}_3\text{O}_4$ -Au nanocrystals and their application for the purification of CD4 lymphocytes, *Biomaterials*, **29**, 4003–4011 (2008)
- Majid S.J., Gassan M.S., Zainab J.T. and Dong L., Iraqi propolis increases degradation of IL-1 $\beta$  and NLRC4 by autophagy following *Pseudomonas aeruginosa* infection, *Microbes and Infection*, **20**, 89-100 (2018)
- Majid S.J., Ali A.T., Usama I.S., Zainab J.T., Ahmed M. and Alyaa S.S., Novel of nano delivery system for linalool loaded on gold nanoparticles conjugated with CALNN peptide for application in drug uptake and induction of cell death on breast cancer cell line, *Materials Science and Engineering C*, **94**, 949-964 (2019)
- O'Neal D.P., Hirsch L.R., Halas N.J., Payne J.D. and West J.L., Photo-thermal tumor ablation in mice using near infrared-absorbing nanoparticles, *Cancer Lett*, **209**, 171–176 (2004)
- Oghabian M.A., Gharehaghaji N., Amirmohseni S., Khoei S. and Guiti M., Detection sensitivity of lymph nodes of various sizes using USPIO nanoparticles in magnetic resonance imaging, *Nanomedicine*, **6(3)**, 496–9 (2010)
- Ruo-Yu H., Jian-Hua L., Shi-Zhong Z., Hong-Zhong L., Ying Zheng M., Ding W. and Dong-Guang W., Preparation and characterization of silica-coated  $\text{Fe}_3\text{O}_4$  nanoparticles used as precursor of ferrofluids, *Applied Surface Science*, **255**, 3485–3492 (2009)
- Tang D., Cui Y. and Chen G., Nanoparticle-based immunoassays in the biomedical field, *Analyst*, **138(4)**, 981–90 (2013)
- Wang Z.Y., Wang L., Zhang J., Li Y.T. and Zhang D.S., A study on the preparation and characterization of plasmid DNA and drug-containing magnetic nanoliposomes for the treatment of tumors, *Int J Nanomedicine*, **6**, 871–5 (2011)

21. Yan S., Zhang D. and Zheng J., Study on the therapeutic effect of Fe<sub>2</sub>O<sub>3</sub> nanometer magnetic fluid hyperthermia on liver cancer, *China Journal of Experimental Surgery*, **21**, 1443–1446 (2004)

22. Yuntao L., Jing L., Yuejiao Z., Jia Z., Ziyu W., Li W., Yanli A., Mei L., Zhiqiang G. and Dongsheng Z., Biocompatibility of Fe<sub>3</sub>O<sub>4</sub> a Au composite magnetic nanoparticles in vitro and in vivo, *Int J Nanomedicine*, **6**, 2805–2819 (2011)

23. You L., Kun W., Yun L., Xin G. and Shizhen Z., Dual docetaxel/superparamagnetic iron oxide loaded nanoparticles for both targeting magnetic resonance imaging and cancer therapy, *Biomaterials*, **32**, 7139-7150 (2011).